Available online at www.sciencedirect.com

ScienceDirect

IFAC PapersOnline CONFERENCE PAPER ARCHIVE

IFAC PapersOnLine 52-26 (2019) 169–174

FBA-based simulator of *Saccharomyces cerevisiae* fed-batch cultures involving an internal unbalanced metabolite

J. Plaza*, Ph. Bogaerts*

* 3BIO-BioControl, Université Libre de Bruxelles,
CP 165/61, 50, Av. F.-D. Roosevelt, B-1050 Brussels, Belgium
(e-mail: jose.plaza.dorado@ulb.ac.be; philippe.bogaerts@ulb.ac.be)

Abstract: A dynamic macroscopic simulator based on Flux Balance Analysis (FBA) is proposed to predict the dynamics of biomass growth, substrate consumption (glucose and ammonium) and ethanol production in *S. cerevisiae* fed-batch cultures. It is based on a metabolic network containing the main metabolism of the yeast, an objective cost function aiming at maximizing the biomass growth, different inequalities corresponding to some biological assumptions such as glucose overflow metabolism and inequalities which link the fluxes to models of substrate uptake rates. Since it was not possible to accurately correlate the input fluxes with only the extracellular species concentration, a new variable is introduced in the uptake rate models using the information at intracellular level. We first determine the dynamics corresponding to the intracellular metabolite, namely alpha-ketoglutarate, and, in a second part, this new information is used for modelling the input flux rates. Secondly, all the information is integrated in a set of mass balances for building a simulator based only on the initial conditions of each species and the feeding rate. It is validated with direct and cross-validation. This model allows, on the one hand, reproducing the dynamics of extracellular species and, on the other hand, describing the accumulation of alpha-ketoglutarate.

Keywords: Saccharomyces cerevisiae, dynamical simulator, Flux Balance Analysis, quasi-steady state.

1. INTRODUCTION

The emerge of genetic engineering, genomics and their technologies has increased the knowledge and understanding of biotechnological processes. In such processes, mathematical modelling plays a key role since it allows control, optimization, design, scale-up and monitoring. Macroscopic models provide a general description of the system without considering the intracellular behavior. They require the choice and validation of macroscopic reaction schemes and the selection of appropriate kinetic models for the reaction rates. Metabolism of microorganisms generates valuable information that can be used for metabolic models as an alternative to the macroscopic models. The main issue of metabolic models is the underdeterminacy, in the sense that the system to be solved generally contains more fluxes to be determined than the available equations (e.g., mass balances of internal metabolites, measured external fluxes). Flux Balance Analysis (FBA) is one of the most effective methods to try to circumvent this problem (Orth, Thiele and Palsson, 2010). This approach uses linear programming to predict metabolic fluxes and is based on the assumption of quasi-steady (Murabito *et al.*, 2009) and the premise of an optimal behavior such as maximum growth rate (Simeonidis *et al.*, 2010). Different models have been used for predicting concentration time profiles of the main extracellular species coupling FBA and ODE's in dynamic FBA models, including mammalian cells (Richelle, Gziri and Bogaerts, 2016; Bogaerts, Mhallem Gziri and Richelle, 2017), *S. cerevisiae* (Plaza and Bogaerts, 2019), CHO cells (Provost *et al.*, 2006) and *E. coli* (Höffner, Harwood and Barton, 2013). Generally, FBA-based simulators use the available external measurements for predicting the uptake rates with extended Monod-laws. There are some efforts to predict the accumulation of intracellular metabolites, such as the study of Baroukh *et al.* (2014), which proposed a dynamic metabolic modeling framework that handles the non-balanced growth condition in the accumulation of lipids and carbohydrates in the microalgae *Tisochrysis lutea*.

In this study we propose an FBA-based simulator for predicting glucose, ammonium, biomass and ethanol concentration time profiles in *S. cerevisiae* fed-batch cultures based on appropriate kinetic models for estimating input uptake rates. We have observed in this case that it is impossible to accurately correlate the input rates with the concentration of extracellular species. For this reason, we use information at intracellular level, namely on the accumulation of alpha-ketoglutarate, and consequently, we have to get rid of the assumption of non-accumulation for that metabolite. The selection of this metabolite is in agreement with the macroscopic model of Richelle, Fickers and Bogaerts (2014), which used the prediction of alpha-ketoglutarate concentration for reproducing the input flux rates, within the same case study.

The original point of this contribution consists in showing how to manage accumulation of internal metabolite based on the input flux rates. The key idea is to describe the dynamics of the metabolite accumulation by using a linear combination of the input fluxes.

10.1016/j.ifacol.2019.12.253

The text is organized as follows: Section 2 presents a brief summary of the FBA-based model proposed by Plaza and Bogaerts (2019). Section 3 proposes the chosen strategy for modeling input uptake rates and the accumulation of alpha-ketoglutarate. Section 4 describes the final FBA-based simulator, the parameter identification procedure and the model validation. Finally, section 5 presents conclusions and perspectives

2. FBA-BASED PREDICTION OF BIOMASS AND ETHANOL CONCENTRATION TIME PROFILES

A FBA-based predictor for biomass and ethanol concentration time profiles in *S. cerevisiae* fed-batch cultures was proposed in Plaza and Bogaerts (2019). The dynamics of the cultures were described with mass balances on each substrate (glucose and ammonium), product (ethanol) and biomass for describing the evolution of their concentrations over the time:

$$\dot{V} = F \quad (1)$$
$$\dot{G} = -v_G X(t) + D(t)\big(G_{feed} - G(t) \big) \quad (2)$$
$$\dot{N} = -v_N X(t) + D(t)(N_{feed} - N(t)) \quad (3)$$
$$\dot{X} = v_x^{opt} X(t) - D(t)X \quad (4)$$
$$\dot{E}_{min} = (v_E(t))_{min}\ X(t) - D(t)E_{min}(t) \quad (5)$$
$$\dot{E}_{max} = (v_E(t))_{max}\ X(t) - D(t)E_{max}(t) \quad (6)$$

where

- D is the dilution rate;
- G, N, X, E_{max} and E_{min} are the concentrations of glucose, ammonium, biomass and ethanol;
- v_G and v_N are the specific uptake rates;
- $(v_E(t))^{min,\ max}$ and $v_X(t)$ are the (minimum and maximum) ethanol production and growth rates;
- G_{feed} and N_{feed} are glucose and ammonium feeding concentrations.

The features of this contribution were:

- use of measured time profiles for the input fluxes (glucose and ammonium);
- 2 inequality constraints for describing glucose overflow metabolism;
- estimation of the biomass composition according to the ammonium feeding rate;
- prediction of v_x^{opt} and $(v_E(t))^{min,\ max}$ by FBA accounting for biomass growth maximization;
- prediction of the concentration time profiles of biomass and ethanol.

For maximizing the biomass, the following linear program (LP) was considered,

$$v_x^{opt}(t_k) = \max_v v_x(t_k)\ \forall t_k \quad (7)$$

under the constraints,

$$Sv = 0; \quad (8)$$
$$S_{in}v \le (1 + e_v)v_{in}(t_k);$$
$$S_{in}v \ge (1 - e_v)v_{in}(t_k);$$
$$A_{ineq}v \ \le b_{ineq};$$

followed by 2 LP's, which allow obtaining the minimum and maximum values of v_E corresponding to biomass maximization:

$$v_E^{MIN,MAX}(t_k) = \underset{v}{\text{Min, Max}}\ v_E\ , \forall t_k \quad (9)$$

under the constraints depicted in Eq. (8) and the additional equality constraint:

$$v_x(t_k) = v_x^{opt}(t_k)\ \forall t_k \quad (10)$$

where $S \in \mathbb{R}^{59x85}$ is the stoichiometric matrix with 59 rows corresponding to the balanced internal metabolites and 85 columns to the metabolic fluxes, $v \in \mathbb{R}^{85}$ the vector of metabolic fluxes, $S_{in} \in \mathbb{R}^{2x85}$ the stoichiometric matrix for glucose and ammonium, $v_{in}^T(t_k) = [v_G\ v_N]$ the consumption rates of glucose and ammonium, e_v the smallest variation coefficient (1% in this work) which allows feasible solutions to the LP {(7),(8),(9)} at each time instant t_k, $A_{ineq}v \le b_{ineq}$ are additional inequality constraints corresponding to some biological assumptions such as glucose overflow metabolism.

More details about the case study, the metabolic network used, the stoichiometric model, the different inequality constraints representing overflow metabolism, biomass composition and FBA-predictor can be found in Plaza and Bogaerts (2019).

3. FROM A MODEL BASED ON UPTAKE FLUX MEASUREMENTS TO A DYNAMICAL SIMULATOR OF *S. CEREVISIAE* FED-BATCH CULTURES

For building a global dynamical simulator, the glucose and ammonium specific uptake rates (v_g and v_n) measurements must be replaced with appropriate kinetic models as those described in Richelle and Bogaerts (2015). Therefore, integrating such models in the set of mass balances {2,3} results in a simulator model able to predict the dynamics of glucose, ammonium, ethanol and biomass. The inputs of the simulator will be: i) the initial conditions of the process (biomass, substrates, products and initial culture volume for starting the process) and ii) the culture medium feeding rate.

3.1 Modelling of substrates input fluxes

As explained before, the information about the input fluxes will be provided through kinetic model structures:

$$v_{in}^T(\vartheta_{in}, t) = [v_G(\vartheta_{in}, t)\ \ v_N(\vartheta_{in}, t)] \quad (11)$$

The usual way to model (11) consists in using the well-known extended-Monod factors:

$$v_{in,k} = \mu_{max,k} \prod_{m \epsilon R_N} \frac{\xi_m}{\xi_m + K_{k\_A\xi_m}} \prod_{l \epsilon P_N} \frac{K_{k\_I\xi_l}}{\xi_l + K_{k\_I\xi_l}} \quad (12)$$

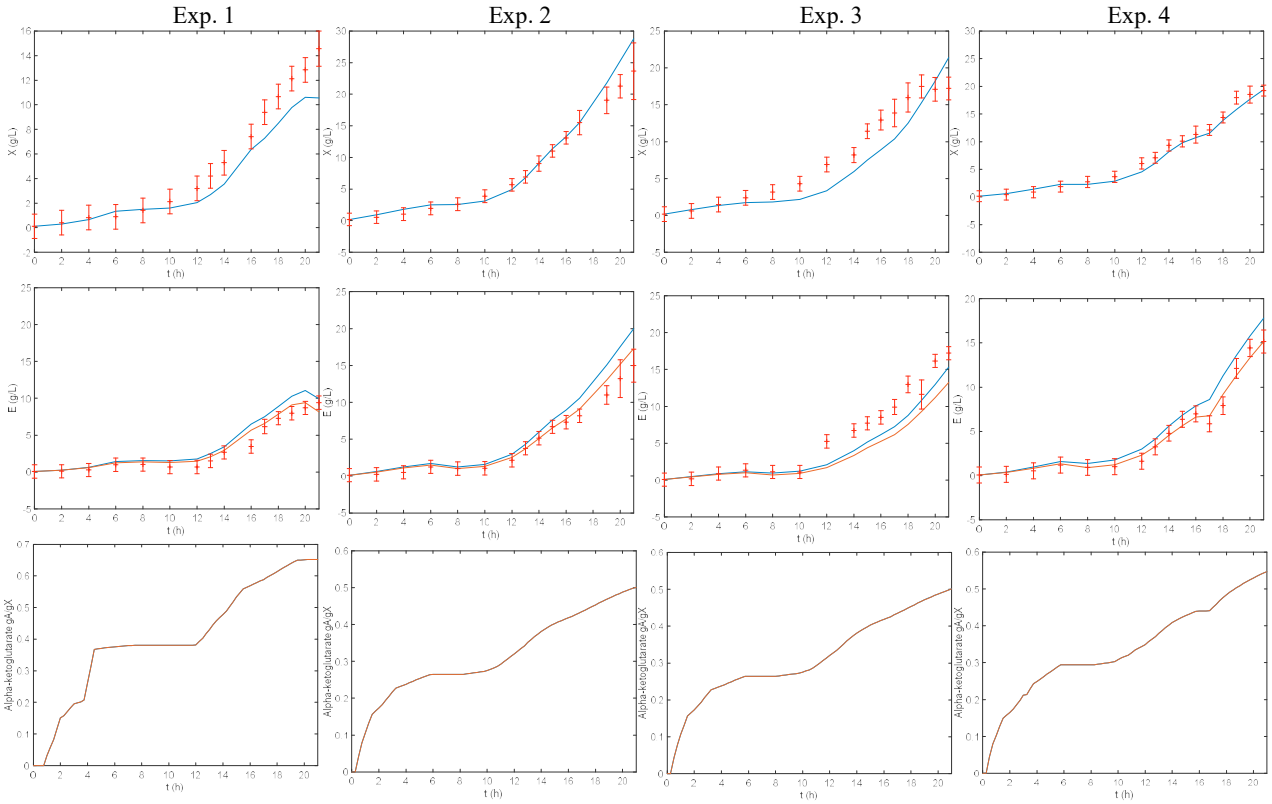

Fig. 1. Direct validation results: in the top, biomass concentration profiles of the 4 experiments, in the medium, maximum (blue) and minimum (red) ethanol concentration profiles of the 4 experiments and in the bottom alpha-ketoglutarate prediction. Comparison of 95 % confidence intervals of the measurements (red bars) with the estimation of the concentration time profiles obtained with the FBA-based model.

where $v_{in,k}$ is the simulated input rate k (glucose or nitrogen), $\mu_{max,k}$ is the maximum specific rate of the input k, $\xi \epsilon \mathbb{R}^N$ is the vector of macroscopic species concentration (G, N, E and X), R_N and P_N are, respectively, the sets of indices of the components which activate and inhibit the input rate k, $K_{k\_A\xi_m}$ and $K_{k\_I\xi_l}$ are respectively a saturation and an inhibition constant of input rate k.

The parameters associated to v_G and v_N are identified by solving the dynamic Eqs. (1)-(6) with Matlab ODE solver *ode15s* and using the Nelder-Mead simplex method (function *fminsearch*) in order to minimize a least squares criterion.

$$J(\theta) = \sum_{j=1}^{n} \sum_{i=1}^{N} (Y_{ij}(\theta) - Y_{mes,ij})^T (W_{ij}^{-1}) (Y_{ij}(\theta) - Y_{mes,ij}) \qquad (13)$$

where θ is the vector of parameters to be identified $\theta^T = [\mu_{max,k}\ K_{k\_AC\xi_m}\ K_{k\_I\xi_l}]$, $Y_{ij}^T(\theta) = [G_{ij}\ N_{ij}]$ is the vector of simulated variables calculated from mass balances (1)-(6) at the i^{th} time instant of the j^{th} experiment, $Y_{mes,ij}^T = [G_{mes,ij}\ N_{mes,ij}]$ is the vector corresponding to the measurements of glucose and nitrogen and W_{ij} is a weighting matrix defined as:

$$W_{ij} = diag(\sigma^2(G_{mes,ij}), \sigma^2(N_{mes,ij})) \qquad (14)$$

where σ^2 are the variances of the corresponding measurement errors. 100 uniformly distributed pseudo- random values over a given range were used as multistart strategy for the initialization of the algorithm to circumvent local minima and convergence problems.

Note that v_x^{opt} and $(v_E(t))^{min,\ max}$ used in (4), (5) and (6) are, at this step of the procedure, the growth and ethanol production rates obtained in Plaza and Bogaerts (2019).

Different model structures have been obtained by trial-and-errors, i.e. testing extended-Monod factors for each external measurement available (results not depicted) without obtaining convincing results that could reproduce adequately the uptake rates. For tackling this problem, we use the information provided at the intracellular level by the alpha-ketoglutarate concentration, which requires to get rid of the assumption of non-accumulation of this metabolite. This is in accordance with the macroscopic model of Richelle, Fickers and Bogaerts (2014), which used such an additional intracellular state variable for the same case study. For doing so, a two-step procedure is implemented: i) dealing with the problem of non-balanced alpha-ketoglutarate (section 3.2) and ii) using the new signal for modeling the substrate input fluxes (section 3.3).

3.2 *Non-balanced alpha-ketoglutarate*

In order to develop a simple model involving alpha ketoglutarate, the following reaction scheme is proposed deduced from Richelle, Fickers and Bogaerts (2014):

$$G \xrightarrow{v_G \le v_{G_{sat}}} X \quad (15)$$

$$G \xrightarrow{v_G > v_{G_{sat}}} X + E + k_{A1}A \quad (16)$$

$$N + k_{A2}A \xrightarrow{v_N} X \quad (17)$$

The alpha-ketoglutarate (A) intracellular species is:

i) produced by glucose during fermentation, in accordance with the assumptions of Aon and Cortassa, (2001) and Richelle, Fickers and Bogaerts (2014);
ii) in a coordinate consumption with nitrogen for producing biomass (Guillamón *et al.*, 2001).

According to the above reaction scheme, alpha-ketoglutarate accumulation is given by:

$$\dot{A} = k_{A1}(v_G - v_{G_{sat}}) - k_{A2}\ v_N \quad (18)$$

Transforming (18) in inequality constraints that can be used in the FBA-model:

$$\begin{aligned} &\textbf{if } \boldsymbol{v_G \le v_{G_{sat}}} \\ &\dot{A} = -k_{A2}\ v_N \\ &\textbf{else} \\ &\dot{A} = k_{A1}(v_G - v_{G_{sat}}) - k_{A2}\ v_N \\ &\textbf{end} \end{aligned} \quad (19)$$

The term corresponding to alpha-ketoglutarate in the stoichiometric model becomes:

$$\dot{A} = S_{alpha} \cdot v\,(t) \quad (20)$$

where $S_{alpha} \epsilon \mathbb{R}_{1x85}$ is the stoichiometric row corresponding to alpha-ketoglutarate.

The new parameters are identified by solving (1)-(6) in combination with (7)-(10), (19) (with measured v_G and v_N) and (20) with Matlab's ODE solver ode15's using the Nelder-Mead simplex method (function *fminsearch*) and the formalism in (13) and (14) but with $\theta^T = [k_{A1}\ \ k_{A2}]$, $Y_{ij}^T(\theta) = [X_{ij}\ E_{ij}]$, $Y_{mes,ij}^T = [X_{mes,ij}\ E_{mes,ij}]$ and $W_{ij} = diag(\sigma^2(X_{mes,ij}), \sigma^2(E_{mes,ij}))$. Results are presented in Table 1 and Fig. 1.

Table 1. Identified values (dim $\vartheta = 2$)

Parameter	Initialization values	Identified Values
k_{A1}	0,001- 1.0	0.0353
k_{A2}	0,001- 1.0	0.0022

3.3 *Substrate input fluxes: using the non-balanced alpha-ketoglutarate*

In the same way as in the beginning of section 3, the input fluxes are modelled using the same procedure, but now using the prediction of alpha-ketoglutarate dynamics of section 3.2. Different model structures have been obtained by trial-and-errors and the following extended-Monod structures are chosen:

$$v_G = \mu_{Gmax}\left(\frac{G}{G+K_1}\right)\left(\frac{X}{X+K_2}\right)\left(\frac{K_3}{AX+K_3}\right) \quad (21)$$

$$v_N = \mu_{Nmax}\left(\frac{N}{N+K_4}\right)\left(\frac{AX}{AX+K_5}\right)\left(\frac{K_6}{AX+K_6}\right) \quad (22)$$

The parameters $\mu_{Gmax}, K_1, K_2, K_3, \mu_{Nmax}, K_4, K_5$ and K_6 are obtained by minimizing a least-squares criterion (13), weighted by the inverse of the measurement error variances (14), comparing the measurement of G and N with their estimations obtained by solving, the ODE's (1)-(6) and (20), using the predictions of v_x^{opt}, $(v_E(t))^{min,\ max}$ and $\dot{A}$ obtained in section 3.2.

The results, obtained after a multi-start strategy with 100 different parameter initial guesses, are presented in Table 2 in Fig. 2.

Table 2. Identified values (dim $\vartheta = 8$)

Parameter	Initialization values	Identified Values
μ_{Gmax}	1- 20	17,9069
K_1	0.01-2	0,5177
K_2	1-5	6,3010
K_3	0.001-0.1	0,0023
μ_{Nmax}	0.1-2	0,7183
K_4	0.01-2	0,4237
K_5	0.001-0.1	0,0161
K_6	0.001-0.1	0,0048

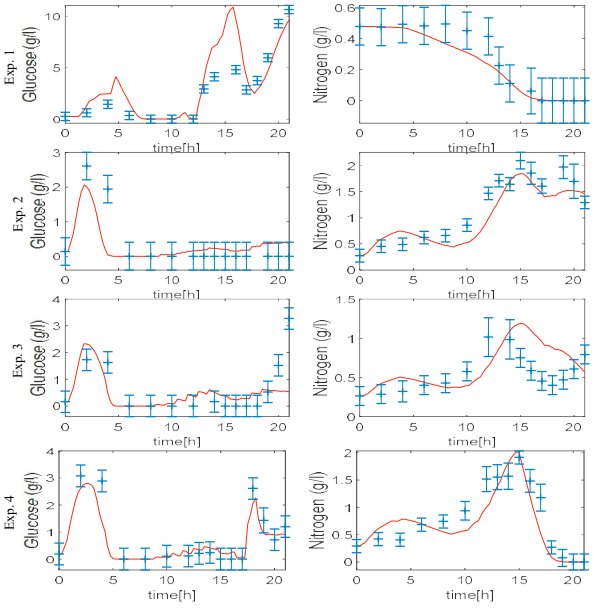

Fig. 2. Comparison of the 95% confidence intervals of the measured concentrations (in blue) with their model estimates (in red) for glucose (at the left) and ammonium (at the right) for the different experiments.

4. DYNAMICAL SIMULATOR OF *S. CEREVISIAE* FED-BATCH CULTURES: FINAL PARAMETER IDENTIFICATION AND VALIDATION

The dynamical simulator of *S. cerevisiae* is described by (1)-(6), (20)-(22), where v_x^{opt} and $(v_E(t))^{min,\,max}$ are determined by solving the FBA problem depicted in (7)-(10), $v_{mes_{in}}(t_k) = [v_G\ v_N]$ is computed with (21) and (22), the dynamics of $\dot{A}$ is given by (19).

In this final step, the parameter values identified for the alpha-ketoglutarate dynamics (Table 1), substrate uptake models (Table 2) and the additional constraints and variable biomass composition (parameters $\alpha_1, \alpha_2, \beta, \gamma, \varepsilon, v_{G_{sat}}, v_{eth}$ identified in Plaza and Bogaerts, 2019) are used as initial values for the optimization algorithm (*fminsearch*) minimizing the sum of squared differences between the simulator outputs and the experimental measurements. This is expressed with the general formalism used in (13) but where $\theta^T = [\alpha_1\ \alpha_2\ \beta\ \gamma\ \varepsilon\ v_{G_{sat}}\ v_{eth}\ k_{A1}\ k_{A2}\ \mu_{Gmax}\ K_1\ K_2\ K_3\ \mu_{Nmax}\ K_4\ K_5\ K_6]$, $Y_{ij}^T(\theta) = [G_{ij}\ N_{ij}\ X_{ij}\ E_{ij}]$ is the vector of simulated variables calculated from mass balances (1)-(6) at the i^{th} time instant of the j^{th} experiment, $Y_{mes,ij}^T = [G_{mes,ij}\ N_{mes,ij}\ X_{mes,ij}\ E_{mes,ij}]$ and $W_{ij} = diag(\sigma^2(G_{mes,ij}), \sigma^2(N_{mes,ij}), \sigma^2(X_{mes,ij}), \sigma^2(E_{mes,ij}))$.

To evaluate the goodness of fit of measured values versus the simulated ones, the linear correlation coefficient (R^2) is computed for each simulated variable in direct and cross validation of the model:

$$R^2 = 1 - \frac{\sum_{j=1}^{n}\sum_{i=1}^{N}(Y_{ij}(\theta) - Y_{mes,ij})^T (Y_{ij}(\theta) - Y_{mes,ij})}{\sum_{j=1}^{n}\sum_{i=1}^{N}(Y_{ij}(\theta) - \overline{Y_{mes,ij}})^T (Y_{ij}(\theta) - \overline{Y_{mes}})} \quad (23)$$

where θ, $Y_{ij}^T(\theta)$, $Y_{mes,ij}^T$ are defined as above and $\overline{Y_{mes}}$ is the mean of the corresponding data points of the different experiments.

Table 3. Parameter values (dim ϑ = 17) identified with all experiments (direct validation) and all sets of 3 experiments (leave-one-out cross validation)

	Exp 1-2-3-4	**Exp 1-2-3**	**Exp 1-2-4**	**Exp 1-3-4**	**Exp 2-3-4**
α_1	0,3227	0,3848	0,4281	0,4051	0,4793
α_2	0,3264	0,4555	0,3344	0,2783	0,4793
β	0,1352	0,1277	0,1269	0,1384	0,1368
γ	0,0569	0,0337	0,0310	0,0805	0,0886
ε	0,1289	0,0639	0,1265	0,1237	0,4793
$v_{G_{sat}}$	0,0017	0,0005	0,0005	0,0033	0,0064
v_{eth}	0,0019	0,0036	0,0003	0,0013	0,0021
k_{A1}	0,0702	0,1652	0,3206	0,0471	0,0830
k_{A2}	0,0021	0,0054	0,0076	0,0025	0,0028
μ_{Gmax}	14,9603	23,7742	35,1657	12,8165	22,5404
K_1	0,2429	0,1547	2,4505	0,3083	0,1281
K_2	1,9232	3,1462	2,5332	1,8192	3,6962
K_3	0,0212	0,0301	0,0445	0,0358	0,0119
μ_{Nmax}	2,8668	2,4464	0,5862	1,9781	0,6808
K_4	1,0308	0,4880	1,5532	0,6289	0,9752
K_5	0,4697	0,4449	0,2223	0,6367	0,0632
K_6	0,0457	0,0393	0,2637	0,0586	0,0423
R^2_G [a]	0,7836	0,7493	0,6110	0,6011	0,6523
R^2_N [a]	0,8920	0,8113	0,8761	0,8915	0,8455
R^2_X [a]	0,9154	0,8984	0,9363	0,9460	0,9339
R^2_E [a]	0,9287	0,9177	0,8640	0,9166	0,9481
SSE [b]	3150,11	3562,08	4331,85	5050,5	10962,4

[a] R^2_G, R^2_N, R^2_X and R^2_E are calculated from Eq. (23) on the whole set of experiments (1-2-3-4).
[b] Sum of squared errors (*SSE*) are calculated from equation (13) on the whole set of experiments (1-2-3-4)

The parameter identification results are presented in Table 3 and Fig. 3 (direct validation and cross validation). Among the 4 available experiments, the 4 existing subsets of 3 experiments have been used for identification procedure (section 3.2 and section 3.3) and, in each case, the remaining experiment has been used for cross-validation. Only the results of the final step of the identification are shown in Table 3.

The simulator gives good predictions for the time profiles of the macroscopic species concentrations, in both direct and cross validation. Moreover, the identified parameter values are in the same range of the initialization values.

This goodness of fit is also confirmed by the regression coefficients which are all greater or equal to 0.81 for ammonium, biomass and ethanol, except for glucose, which had a lower value of 0.78 in direct validation and 0.60 in cross validation. This is due to the dynamics of glucose which is not well captured in the beginning of experiment 1. Regarding the SSE, the values have the same order of magnitude computed on all sets of experiments (Table 3), except for the set of experiments 2-3-4. This latter can be explained since the experiment 1 is the one which has the information regarding nitrogen limitation conditions.

5. CONCLUSIONS AND PERSPECTIVES

This contribution introduces an FBA-based dynamical simulator of fed-batch cultures of *S. cerevisiae,* which allows to predict the dynamics of extracellular species and one intracellular metabolite. The FBA-based model is based on:

- models of the substrate specific uptake rates,
- inequality constraints for explaining glucose overflow metabolism,
- an objective cost function accounting for biomass growth maximization,
- biomass composition as a function of the presence or absence of ammonium concentration in the feeding rate,
- one internal metabolite which is assumed to be unbalanced.

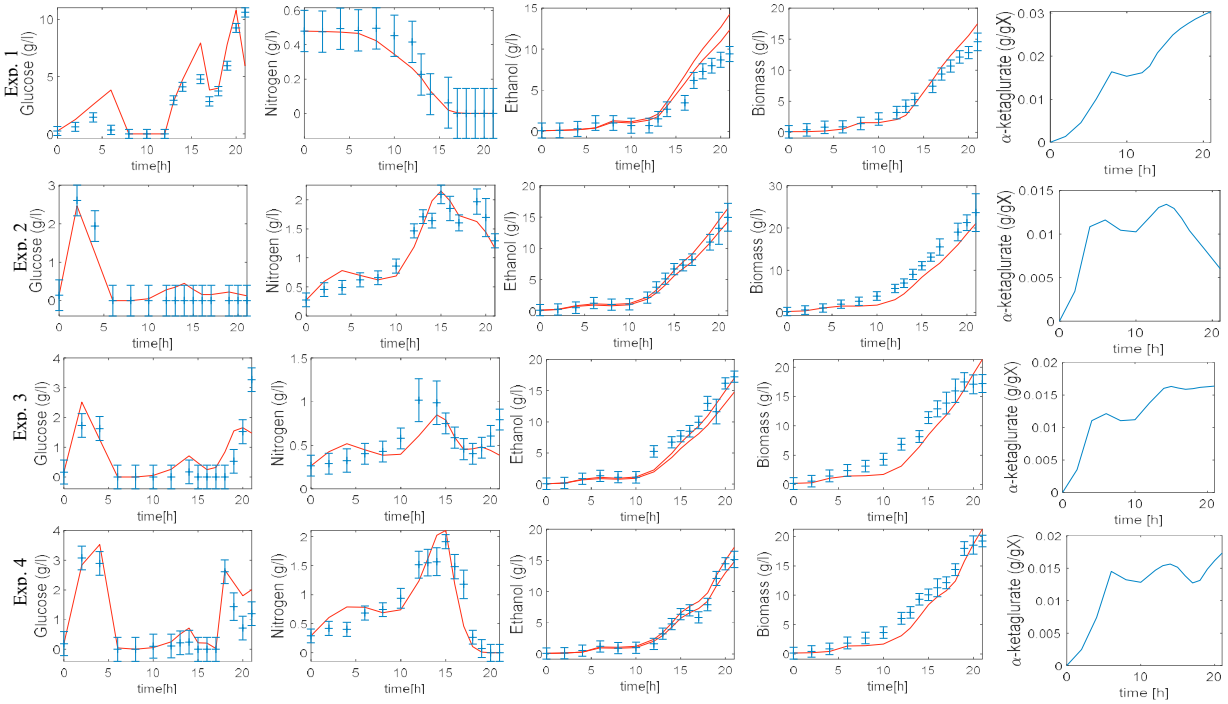

Fig. 3. Comparison between model simulation and measurements of the 4 experiments (direct validation). Comparison of 95 % confidence intervals of the measurements (blue bars) with the estimation of the concentration time profiles obtained with the FBA-based simulator

The final simulator has a structural complexity of 17 parameters. The identified model successfully reproduces the biomass, substrates and product concentration time profiles in direct and cross-validation.

This work allows to build a biological culture simulator which efficiently predicts external substrates consumption, biomass and metabolites production based on a metabolic network and constrained dynamic FBA.

The sensitivity of model outputs with respect to parameters will be analyzed, possibly leading to a model reduction. In addition, the work presented here could be described in a systematic methodology and applied to other possible intracellular metabolites.

REFERENCES

Aon, J. C. and Cortassa, S. (2001) 'Involvement of Nitrogen Metabolism in the Triggering of Ethanol Fermentation in Aerobic Chemostat Cultures of Saccharomyces cerevisiae', *Metabolic Engineering*, 3(3), pp. 250–264. doi: 10.1006/mben.2001.0181.

Baroukh, C. *et al.* (2014) 'DRUM: A New Framework for Metabolic Modeling under Non-Balanced Growth. Application to the Carbon Metabolism of Unicellular Microalgae', *PLoS ONE*. Edited by A. Vertes, 9(8), p. e104499. doi: 10.1371/journal.pone.0104499.

Bogaerts, Ph., Mhallem Gziri, K. and Richelle, A. (2017) 'From MFA to FBA: Defining linear constraints accounting for overflow metabolism in a macroscopic FBA-based dynamical model of cell cultures in bioreactor', *Journal of Process Control*. Elsevier Ltd, 60, pp. 34–47. doi: 10.1016/j.jprocont.2017.06.018.

Guillamón, J. M. *et al.* (2001) 'The glutamate synthase (GOGAT) of Saccharomyces cerevisiae plays an important role in central nitrogen metabolism', *FEMS Yeast Research*, 1(3), pp. 169–175. doi: 10.1016/S1567-1356(01)00034-4.

Höffner, K., Harwood, S. M. and Barton, P. I. (2013) 'A reliable simulator for dynamic flux balance analysis', *Biotechnology and Bioengineering*, 110(3), pp. 792–802. doi: 10.1002/bit.24748.

Murabito, E. *et al.* (2009) 'Capturing the essence of a metabolic network: A flux balance analysis approach', *Journal of Theoretical Biology*. Elsevier, 260(3), pp. 445–452. doi: 10.1016/j.jtbi.2009.06.013.

Orth, J. D., Thiele, I. and Palsson, B. Ø. (2010) 'What is flux balance analysis?', *Nature Biotechnology*. Nature Publishing Group, 28(3), pp. 245–248. doi: 10.1038/nbt.1614.

Plaza, J. and Bogaerts, Ph. (2019) 'Fba-Based Prediction of Biomass and Ethanol Concentration Time Profiles in Saccharomyces cerevisiae Fed-Bath Cultures', *IFAC-PapersOnLine*, 52(1), pp. 82–87. doi: 10.1016/j.ifacol.2019.06.041.

Provost, A. *et al.* (2006) 'Metabolic design of macroscopic bioreaction models: Application to Chinese hamster ovary cells', *Bioprocess and Biosystems Engineering*, 29(5–6), pp. 349–366. doi: 10.1007/s00449-006-0083-y.

Richelle, A. and Bogaerts, Ph. (2015) 'Systematic methodology for bioprocess model identification based on generalized kinetic functions', *Biochemical Engineering Journal*. Elsevier B.V., 100(August), pp. 41–49. doi: 10.1016/j.bej.2015.04.003.

Richelle, A., Fickers, P. and Bogaerts, Ph. (2014) 'Macroscopic modelling of baker's yeast production in fed-batch cultures and its link with trehalose production', *Computers & Chemical Engineering*. Elsevier Ltd, 61(February), pp. 220–233. doi: 10.1016/j.compchemeng.2013.11.007.

Richelle, A., Gziri, K. M. and Bogaerts, Ph. (2016) 'A methodology for building a macroscopic FBA-based dynamical simulator of cell cultures through flux variability analysis', *Biochemical Engineering Journal*, 114, pp. 50–64. doi: 10.1016/j.bej.2016.06.017.

Simeonidis, E. *et al.* (2010) 'Why does yeast ferment? A flux balance analysis study', *Biochem Soc Trans*, 38(5), pp. 1225–1229. doi: 10.1042/BST0381225.